The subcellular localization of flag-epitope and Rab7 was almost identical, indicating that Rab7N125I was expressed as a flag-fusion protein as expected. Although the cells expressing Rab7N125I were fewer than those expressing Rab7wt, they could clearly be distinguished from the non-expressing control by the immunofluorescence. From these results, it seems that the amount of Rab7N125I was smaller than that of Rab7wt because of the lower transfection efficiency of the Rab7N125I plasmid.

Subcellular localization of Rab7N125I was distinct from that of wild-type protein in COS7 cells In order to examine the expression and subcellular distribution of flag-fused Rab7 proteins in COS7 cells, we carried out immunofluorescent staining of the cells and observed them with a confocal laser scanning microscope. All images were taken in such a way that exogenous Rab7-expressing cells and untransfected control cells were obtained in every image. Rab7wt-positive granules were aggregated in the perinuclear area and rarely detected in the cell periphery (Fig 2*A-C*). Some of the Rab7wt-positive granules appeared to form vesicular structures (Fig 2*B, inset*). In contrast, in cells expressing Rab7N125I, the mutant protein was detected in both the cytoplasmic and the perinuclear areas (Fig 2*D-F*). Small immuno-positive granules were diffusely scattered throughout the cytoplasm, including its dendrites. Swollen Rab7N125I-positive granules were conglomerated in the perinuclear area without vesicular appearance.

To confirm the localization of the exogenous Rab7 proteins, cells were doubly stained with anti-flag polyclonal antibody and organelle marker antibody, anti-p230

trans Golgi mAb (Fig 2*A, D*) for TGN, anti-EEA1 mAb (Fig 2*B, E*) for early endosomes, and anti-MPR mAb (Fig 2*C, F*) for late endosomes. Rab7wt was co-localized with MPR, but not with p230 trans Golgi or EEA1. The distribution of each organelle marker in Rab7wt-expressing cells was similar to that in control cells (Fig 2*A-C*). In contrast, the two forms of Rab7N125I-positive granules, located in the perinuclear area and the cytoplasm, were partly co-localized with EEA1 (Fig 2*E*, *inset*). Some of the conglomerated granules were aggregated in TGN area, perturbing the TGN distribution (Fig 2*D*). There was not any co-localization of Rab7N125I with MPR, and the distribution of MPR in the Rab7N125-expressing cells was similar to that of the control cells (Fig 2*F*). These results indicate that Rab7N125I was not localized to late endosomes but was partly co-localized with EEA1-positive early endosomes, whereas Rab7wt was localized to late endosomes.

Rab7N125I-positive granules maintained interaction with depolymerized microtubule fragments. One of the effecter molecules of Rab7, Rab-interacting lysosomal protein (RILP), interacts only with GTP-bound Rab7 and recruits dynein-dynactin motors and regulates the minus-end-directed organelle transport toward the microtubule-organizing center (MTOC) (Cantalupo *et al*, 2001; Jordens *et al*, 2001). To study the relationship between Rab7 and microtubules, COS7 cells were transfected with the Rab7wt or Rab7N125I plasmid and incubated in the presence or absence of a microtubule-disrupting agent, nocodazole, prior to the fixation. Rab7wt-positive granules were assembled around MTOC where microtubules showed convergence, forming enlarged ring-shaped vesicles (Fig 3*A*).

After the nocodazole treatment, Rab7wt-positive granules were dispersed in the cytoplasm and did not show the ring-shaped appearance (Fig 3*B*). Rab7N125I-positive granules throughout the cytoplasm were attached to the non-depolymerized microtubules (Fig 3*C, inset*). In contrast to Rab7wt, the majority of Rab7N125I was co-localized with α-tubulin after the depolymerization of microtubules (Fig 3*D*). The conglomerated perinuclear granules did not change in shape or distribution even after the nocodazole treatment.

Rab7N125I inhibited the localization of TYRP1, which was quite different from that of TYR or gp100. To study how Rab7 is involved in the localization of melanosomal proteins, melan-a, an immortal murine melanocyte cell line, cells were transfected with the plasmids encoding Rab7wt or Rab7N125I, and double-immunofluorescent staining was carried out by using anti-flag polyclonal antibody and HMSA5 for TYRP1 (Fig 4*A, D*), anti-flag mAb and PEP7 antiserum for TYR (Fig 4*B, E*), and anti-flag polyclonal antibody and HMB45 for gp100 (Fig 4*C, F*). TYRP1-positive granules in both Rab7wt-expressing and control cells were similarly distributed; densely aggregated in the perinuclear area and sparsely in the peripheral area (Fig 4*A*). The majority of the perinuclear TYRP1 was co-localized with Rab7wt (Fig 4*A*, *inset*). In contrast to the cells expressing Rab7wt, TYRP1 was not detected in the entire cytoplasm of the cells expressing Rab7N125I (Fig 4*D*).

The TYR-positive granules in Rab7wt-expressing cells and control cells were also distributed in both the perinuclear and peripheral areas (Fig 4*B*). The co-localization of TYR with Rab7wt was less apparent than that of TYRP1 with

Rab7wt (Fig 4*B*, *inset*). Unlike TYRP1 which was not detectable in the Rab7N125I-expressing melan-a cells, TYR-positive granules were observed in the Rab7N125I-expressing cells. However, TYR-positive granules in the Rab7N125I-expressing melan-a cells did not show perinuclear aggregation (Fig 4*E*).

The gp100-positive granules in Rab7wt-expressing cells and control cells were also distributed in both the perinuclear and peripheral areas (Fig 4*C*). The gp100-positive granules in the perinuclear area were partially co-localized with Rab7wt (Fig 4*C*, *inset*). The cells expressing Rab7N125I contained a comparable amount of gp100-positive granules to those expressing Rab7wt. The majority of gp100-positive granules in the Rab7N125I-expressing cells were distributed in the peripheral area of the cytoplasm (Fig 4*F*).

Rab7N125I altered the melanosomal protein expression and distribution To verify that the distribution of the melanosomal proteins is altered by Rab7N125I expression in melan-a cells, the microscopic features of immunostains in melan-a cells were statistically analyzed (Fig 5). Melan-a cells were transfected with the plasmids encoding Rab7wt or Rab7N125I and stained with anti-flag antibodies together with HMSA5 for TYRP1, PEP7 antiserum for TYR or HMB45 for gp100. Approximately 68 digital images (ranging 55-75 images) of the cells expressing exogenous Rab7 were examined for each analysis. The distribution of TYRP1-, TYR- and gp100-positive granules was categorized into three basic patterns; *perinuclear*, cells had perinuclearly aggregated granules; *peripheral*, cells had no perinuclear aggregated granules but peripherally scattered granules; *no granules*,

cells had no granules.

The distribution pattern of TYRP1-positive granules in Rab7N125I-expressing cells was quite different from that of Rab7wt-expressing cells (Fig 5*A*, $p<0.00001$). In 73.1% of Rab7N125I-expressing cells, TYRP1-positive granules were not detected. From among the remaining cells (26.9%), which were categorized as *perinuclear* or *peripheral* pattern cells, 23.9% contained a smaller number of TYRP1-positive granules than did control cells, and only 3.0% of the cells contained a comparable number of TYRP1-positive granules to control cells (data not shown).

In contrast, the percentage of cells without detectable TYR-positive granules was 13.9% and 14.7% in the cells expressing Rab7wt and Rab7N125I, respectively (Fig 5*B*). The percentage of cells showing TYR with *perinuclear* pattern in Rab7wt- and Rab7N125I-expressing cells was 58.3% and 37.3%, respectively. The percentage of cells showing TYR with *peripheral* pattern in Rab7wt- and Rab7N125I-expressing cells was 27.8% and 48.0%, respectively. The difference in the distribution patterns of TYR between Rab7wt- and Rab7N125I-expressing cells was not statistically significant ($p=0.025$).

The percentage of cells without detectable gp100-positive granules was 7.1% and 7.3% in the cells expressing Rab7wt and Rab7N125I, respectively (Fig 5*C*). The percentage of cells showing gp100 with *perinuclear* pattern in Rab7wt- and Rab7N125I-expressing cells was 67.1% and 25.5%, respectively. And the percentage of cells showing gp100 with *peripheral* pattern in Rab7wt- and Rab7N125I-expressing cells was 25.7% and 67.3%, respectively. The difference in the distribution patterns of TYR-positive granules between Rab7wt- and

Rab7N125I-expressing cells was statistically significant ($p<0.00001$). These results indicate that Rab7N125I affects the trafficking of TYR, TYRP1 and gp100 differently and, among them, TYRP1 required Rab7 function for its transport.

Discussion

TYR, TYRP1 and gp100 are melanosomal proteins that possess distinct biological and biochemical functions in the melanogenesis cascade. They are all glycoproteins and are sorted from Golgi compartment to melanosomes. A previous study indicated that TYR, TYRP1 and TYRP2 form a melanogenic complex in low pH circumstance (Orlow *et al*, 1994). A more recent study indicated that TYR and TYRPs form a complex in late endosomes and are transported to stage II melanosomes (Jimbow *et al*, 2000). However, it is still unknown whether TYR and TYRPs travel together in the same or independent pathways from TGN to early-stage melanosomes (Richmond *et al,* 2005). The present study using Rab7wt and its dominant negative mutant showed that the vesicular transport of TYRP1 from Golgi compartment to melanosomes is different from that of TYR and gp100, as disclosed by comparison of the bio-distribution of these melanosomal proteins. Rab7wt detected as perinuclear aggregates was localized at late endosomes and did not alter the pre-existing subcellular structures, while Rab7N125I altered the distribution of Rab7-positive granules and perturbed endosomal vesicular transport, specifically inhibiting a proper distribution of TYRP1. Most of the melan-a melanocytes expressing Rab7N125I contained no or reduced number of TYRP1-positive granules. Although 3.0% of the Rab7N125I-expressing cells contained a comparable number of

TYRP1-positive granules to control cells, the expression level of Rab7N125I in these minority cells was lower than in other Rab7N125I-expressing ones (data not shown). Therefore the melan-a cells expressing Rab7N125I appeared to lose TYRP1 immunoreactivity. These findings indicate that TYRP1 may pass through early and late endosomal compartments before being targeted to melanosomes, and that the transport pathway of TYRP1 from Golgi compartment to melanosomes is different from that of TYR and gp100.

A previous study indicated that for proper targeting of TYR, di-leucine-based signal motif at the cytoplasmic domain of TYR , to which AP-3 binds, and two acidic amino acid residues four to five proximal to the di-leucine motif are essential (Huizing *et al*, 2001). However, TYRP1 possesses only one of the two acidic amino residues, revealing less affinity to AP-3 than TYR. It was also reported that TYRP1 resides in the transport vesicles with AP-1 (Raposo *et al*, 2001). The AP-1 is involved in the TGN/endosome trafficking while AP-3 regulates the vesicular transport to lysosome-related organelles including melanosomes (Robinson, 2004). Therefore it can be postulated that TYR is transported from TGN to early-stage melanosomes directly or indirectly via late endosomes by AP-3, and that TYRP1 is transported to early endosomes, then subsequently to late endosomes under the regulation of Rab7, and finally to early-stage melanosomes. TYR and TYRPs may form a complex after reaching late endosomal/melanosomal compartments which have an acidic environment.

It has been reported that RILP, one of the effecter molecules of Rab7, recruits dynein-dynactin motors and regulates the organelle transport toward MTOC

(Cantalupo *et al*, 2001; Jordens *et al*, 2001). Actually, Rab7wt expressed in COS7 formed vesicular structures around MTOC. Interestingly, Rab7N125I-positive granules also appeared to interact with microtubules. The granules with Rab7N125I may interact more stably than those with Rab7wt because Rab7N125I was co-localized even with disrupted microtubule fragments. It is possible that Rab7N125I also interacts with RILP and binds the organelle to microtubules while the minus-end directed motility of the organelle is inhibited by the dominant negative effect. Another Rab7-binding protein, hVPS34, has also been reported to bind with Rab7N125I more tightly than Rab7wt, but Rab7N125I-bound hVPS34 has reduced phosphatidylinositol 3'-kinase activity compared with the Rab7wt-bound counterpart (Stein *et al*, 2003). On the other hand, the conglomerated Rab7N125I-positive granules were localized in the perinuclear area even after nocodazole treatment. They were distributed in the perinuclear area without polarity while Rab7wt-positive granules were assembled around MTOC. These conglomerated structures may have been caused by an excessive amount of mutant proteins that exhaust the partners, RILP and/or dynein-dynactin complex, and were accumulated in the perinuclear area by certain microtubule-independent transport machinery.

The majority of the gp100-positive granules in Rab7N125I-expressing cells were peripherally distributed. It has been reported that gp100 is sorted initially to the earliest form of melanosomes derived from the endoplasmic reticulum/Golgi compartment (Jimbow *et al*, 2000; Yasumoto *et al*, 2004). However it has also been reported that gp100-positive early-stage melanosomes are the unique component of endosomal lineage granules (Raposo et al, 2001). Our present results may support

the former hypothesis as Rab7N125I expression affected the dispersion of gp100-positive granules in the perinuclear areas and did not appear to alter the gp100 transport to melanosomes locating in the peripheral area of the cytoplasm. Early-stage melanosomes possess bi-directional motility on microtubules until they are caught by the peripheral actomyosin system (Wu *et al*, 1998). Rab7 is localized on the melanosomal membrane (Gomez *et al*, 2001). RILP recruits dynein-dynactin motor complex onto late endosomes and lysosomes (Jordens et al, 2001). Melanocytes treated with a cytoplasmic dynein antisense oligonucleotide demonstrated transport of melanosomes into dendrites (Byers *et al*, 2000). Taking these reports into consideration, Rab7 may also function as a regulator of minus-end directed movement of gp100-positive early-stage melanosomes by interacting with RILP and regulating the dynein-dynactin complex on the melanosomal membrane.

In this study the transfection efficiency of Rab7N125I was quite lower than that of Rab7wt in both COS7 and melan-a. The sequence of the plasmid encoding Rab7N125I is identical to that encoding Rab7wt, with the exception of only one point mutation which makes the single amino acid substitution of N125I in Rab7. Moreover, the mutant protein appeared to be expressed in COS7 cells without unexpected modification. Therefore the lower transfection efficiency of Rab7N125I compared to Rab7wt may be intrinsic to the mutant protein. It has been reported that the dominant negative form of Rab27a, another Rab member protein, was more rapidly degraded than wild-type protein when it was overexpressed in COS7 cells (Ramalho *et al*, 2002). It is also possible that the cells expressing Rab7N125I were rarely visualized by immunofluorescent staining because of the rapid degradation of

mutant protein, and we might be able to detect the cells expressing mutant Rab7 that fortunately escaped from the degradation system owing to specific conditions such as a certain phase in the cell cycle. It seems that the transient expression and immunofluorescent observation is a useful approach to detect the effect of mutant Rab7 on the transport of melanosomal proteins.

Recently, amino acid substitutions of L129F and V162M in Rab7 have been reported to cause Charcot-Marie-Tooth type 2B (CMT2B) neuropathy (Verhoeven *et al*, 2003). CMT2B is marked by sensory and motor neuron impairment, distal muscle weakness and atrophy, and skin ulceration. Although the Leu129 residue of Rab7 is located quite close to the GTP/GDP binding domain, it has not been reported that CMT2B reveals hypo-pigmented symptoms. However, there is a possibility that the individuals who possess Rab7 mutation only reveal subtle skin color change because affected melanosomal protein is restricted to TYRP1. In fact, the oculocutaneous albinism type-3 patients who have the only TYRP1 mutation reveal subtle skin-color change (Boissy *et al*, 1996). There is also another possibility that L129F in Rab7 is only a rare polymorphism, because some patients in one pedigree of CMT2B had the mutation of L129F but the other patients in the same pedigree did not have the mutation (Verhoeven *et al*, 2003).

In conclusion, this report demonstrates that the transport pathway of TYRP1 from Golgi complex to melanosomes may be different from that of TYR and gp100 and that Rab7 is a crucial regulator of TYRP1 transport. These results may indicate that Rab7 and/or its descendants are potent regulators of endosomal vesicular trafficking in melanogenesis and that they can be candidates for responsibility for as

yet unidentified abnormal melanin pigmentation disease.

Acknowledgments

We thank Dr D. C. Bennett (St. George's Hospital Medical School, London, UK) for melan-a cells, and Dr V. J. Hearing (NIH, Bethesda, MD) for providing us with anti-PEP7 antiserum. This work was supported in part by Grants-in-Aid for Cancer Research from the Ministry of Health, Labour and Welfare, and for Scientific Research from the Ministry of Education, Culture, Sports, Science and Technology of Japan.

References

Boissy RE, Zhao H, Oetting WS *et al*: Mutation in and lack of expression of tyrosinase-related protein-1 (TRP-1) in melanocytes from an individual with brown oculocutaneous albinism: a new subtype of albinism classified as "OCA3". Am J Hum Genet 58:1145-1156, 1996

Bucci C, Thomsen P, Nicoziani P, McCarthy J, van Deurs B: Rab7: A key to lysosome biogenesis. Mol Biol Cell 11:467-480, 2000

Byers HR, Yaar M, Eller MS, Jalbert NL, Gilchrest BA: Role of cytoplasmic dynein in melanosome transport in human melanocytes. J Invest Dermatol 114:990-997, 2000

Cantalupo G, Alifano P, Roberti V, Bruni CB, Bucci C: Rab-interacting lysosomal protein (RILP): the Rab7 effector required for transport to lysosomes. EMBO J 20:683-693, 2001

Chavrier P, Parton RG, Hauri HP, Simons K, Zerial M: Localization of low molecular weight GTP binding proteins to exocytic and endocytic compartments. Cell 62:317-329, 1990

Der JE, Dixon WT, Jimbow K, Horikoshi T: A murine monoclonal antibody, MoAb HMSA-5, against a melanosomal component highly expressed in early stages, and common to normal and neoplastic melanocytes. Br J Cancer 67:47-57, 1993

Dong J, Chen W, Welford A, Wandinger-Ness A: The proteasome alpha-Subunit XAPC7 interacts specifically with Rab7 and late endosomes. J Biol Chem 279:21334-21342, 2004

Feng Y, Press B, Wandinger-Ness A: Rab 7: an important regulator of late endocytic

membrane traffic. J Cell Biol 131:1435-1452, 1995

Gomez PF, Luo D, Hirosaki K, et al: Identification of rab7 as a melanosome associated protein involved in the intracellular transport of tyrosinase related protein-1. J Invest Dermatol 117:81-90, 2001

Gutierrez MG, Munafo DB, Beron W, Colombo MI: Rab7 is required for the normal progression of the autophagic pathway in mammalian cells. J Cell Sci 117:2687-2697, 2004

Hirosaki K, Yamashita T, Wada I, Jin HY, Jimbow K: Tyrosinase and tyrosinase-related protein 1 require Rab7 for their intracellular transport. J Invest Dermatol 119:475-480, 2002

Huizing M, Sarangarajan R, Strovel E, Zhao Y, Gahl WA, Boissy RE: AP-3 mediates tyrosinase but not TRP-1 trafficking in human melanocytes. Mol Biol Cell 12:2075-2085, 2001

Jackson IJ: Homologous pigmentation mutations in human, mouse and other model organisms. Hum Mol Gen 6:1613-1624,1997

Jimbow K, Chen H, Gomez PF *et al*: Intracellular vesicular trafficking of tyrosinase gene family protein in eu- and pheomelanosome biogenesis. Pigment Cell Res 13:110-117, 2000

Jimenez-Cervantes C, Solano F, Kobayashi T, Urabe K, Hearing VJ, Lozano JA, Garcia-Borron JC: A new enzymatic function in the melanogenic pathway. The 5,6-dihydroxyindole-2-carboxylic acid oxidase activity of tyrosinase-related protein-1 (TRP1). J Biol Chem 269:17993-8000, 1994

Jordens I, Fernandez-Borja M, Marsman M *et al*: The Rab7 effector protein RILP

controls lysosomal transport by inducing the recruitment of dynein-dynactin motors. Curr Biol 11:1680-1685, 2001

Meresse S, Gorvel JP, Chavrier P: The Rab7 resides on a vesicular compartment connected to lysosomes. J Cell Sci 108:3349-3358, 1995

Mizuno K, Kitamura A, Sasaki T: Rabring7, a novel Rab7 target protein with a RING finger motif. Mol Biol Cell 14:3741-3752, 2003

Oetting WS, King RA: Molecular basis of albinism: mutations and polymorphisms of pigmentation genes associated with albinism. Hum Mutat 13:99-115, 1999

Orlow SJ, Zhou BK, Chakraborty AK, Drucker M, Pifko-Hirst S, Pawelek JM: High-molecular-weight forms of tyrosinase and the tyrosinase-related proteins: evidence for a melanogenic complex. J Invest Dermatol 103:196-201, 1994

Press B, Feng Y, Hoflack G, Wandinger-Ness A: Mutant Rab7 causes the accumulation of cathepsin D and cation-independent mannose 6-phosphate receptor in an early endocytic compartment. J Cell Biol 140:1075-1089, 1998

Ramalho JS, Anders R, Jaissle GB, Seeliger MW, Huxley C, Seabra MC: Rapid degradation of dominant-negative Rab27 proteins *in vivo* precludes their use in transgenic mouse models. BMC Cell Biol 3:26, 2002

Raposo G, Tenza D, Murphy DM, Berson JF, Marks MS: Distinct protein sorting and localization to premelanosomes, melanosomes, and lysosomes in pigmented melanocytic cells. J Cell Biol 152:809-823, 2001

Richmond B, Huizing M, Knapp J, Koshoffer A, Zhao Y, Gahl WA, Boissy RE: Melanocytes derived from patients with hermansky-pudlak syndrome types 1, 2, and 3 have distinct defects in cargo trafficking. J Invest Dermatol 124: 420-427,

2005

Robinson MS: Adaptable adaptors for coated vesicles. Trends Cell Biol 4:167-174, 2004

Stein MP, Feng Y, Cooper KL, Welford AM, Wandinger-Ness A: Human VPS34 and p150 are Rab7 interacting partners. Traffic 4:754-771, 2003

Verhoeven K, Jonghe PD, Coen K *et al*: Mutations in the small GTP-ase late endosomal protein RAB7 cause Charcot-Marie-Tooth type 2B neuropathy. Am J Hum Genet 72:722-727, 2003

Vieira OV, Bucci C, Harrison RE *et al*: Modulation of Rab5 and Rab7 recruitment to phagosomes by phosphatidylinositol 3-kinase. Mol Cell Biol 23:2501-2514, 2003

Vitelli R, Santillo M, Lattero D, Chiariello M, Bifulco M, Bruni CB, Bucci C: Role of the small GTPase Rab7 in the late endocytic pathway. J Biol Chem 272:4391-4397, 1997

Wu X, Bowers B, Rao K, Wei Q, Hammer JA3rd: Visualization of melanosome dynamics within wild-type and dilute melanocytes suggests a paradigm for myosin V function *in vivo*. J Cell Biol 143:1899-1918, 1998

Yasumoto K, Watabe H, Valencia JC, Kushimoto T, Kobayashi T, Appella E, Hearing VJ: Epitope mapping of the melanosomal matrix protein gp100 (PMEL17): rapid processing in the endoplasmic reticulum and glycosylation in the early Golgi compartment. J Biol Chem 279:28330-28338, 2004

Figure legends

Figure 1. Flag-fused Rab7 proteins in COS7 were characterized. (*A*) COS7 cells expressing exogenous Rab7wt and Rab7N125I were lysed, immunoprecipitated by using anti-Flag M2 affinity gel, resolved by SDS-PAGE, and analyzed by immunoblot with anti-flag polyclonal antibody. (*B*) Transfection efficiency of the plasmid encoding Rab7wt or Rab7N125I in COS7 cells was examined. The percentage of flag-positive cells in approximately 100 cells depicted in a microscopic digital image was calculated. Bars are means ± SD of four different images. (*C-E*) COS7 cells transfected with the plasmid encoding Rab7N125I were stained with anti-flag M2 mAb (*C*) and Rab7 antiserum (*D*). *E* shows a merged image of *C* and *D*. Results show one representative experiment of three. Scale bar= 10 μm. wt, Rab7wt; N125I, Rab7N125I.

Figure 2. Rab7wt was localized to late endosomes whereas Rab7N125I was distributed in the perinuclear area as well as throughout the cytoplasm. COS7 cells transfected with the plasmid encoding Rab7wt (*A-C*) or Rab7N125I (*D-F*) were stained with anti-flag antibody (*green*) and subcellular marker antibody (*red*); anti-p230 trans Golgi (*A, D*), anti-EEA1 (*B, E*) and anti-MPR (*C, F*). Arrowheads point to Rab7wt-positive vesicular structures. Arrows point to Rab7N125I-positive granules which were co-localized with EEA1. Results show one representative experiment of three. Scale bars= 10 μm.

Figure 3. Rab7N125I-positive granules interacted with microtubule. COS7

cells expressing Rab7wt (*A, B*) or Rab7N125I (*C, D*) were incubated for 30 minutes in the presence (*A, C*) or absence (*B, D*) of nocodazole prior to fixation. Cells were stained with anti-flag antibody (*green*) and anti-α-tubulin antibody (*red*). Results show one representative experiment of three. Scale bars= 10 μm; Noc, nocodazole treatment.

Figure 4. Rab7N125I inhibited the localization of TYRP1, which was quite different from that of TYR or gp100. Melan-a cells transfected with the plasmid encoding Rab7wt (*A-C*) or Rab7N125I (*D-F*) were stained with anti-flag antibody (*green*) and antibody against melanosomal proteins (*red*); anti-TYRP1 (*A, D*), anti-TYR (*B, E*) or anti-gp100 (*C, F*) antibody. Results show one representative experiment of three. Scale bars= 10 μm.

Figure 5. Rab7N125I altered the distribution of melanosomal proteins. For each statistical analysis, the immunofluorescent images of Rab7wt- or Rab7N125I-expressing cells were collected. The distribution of melanosomal protein-positive granules in the cells was categorized into three basic patterns; *PN*, *perinuclear*; *PP*, *peripheral*; *NG*, *no granules*. Bars are percentages of the cells included in each category. The total number of cell examined is shown in parentheses. *A*, $p<0.00001$; *B*, $p=0.025$; *C*, $p<0.00001$; wt, Rab7wt; N125I, Rab7N125I.

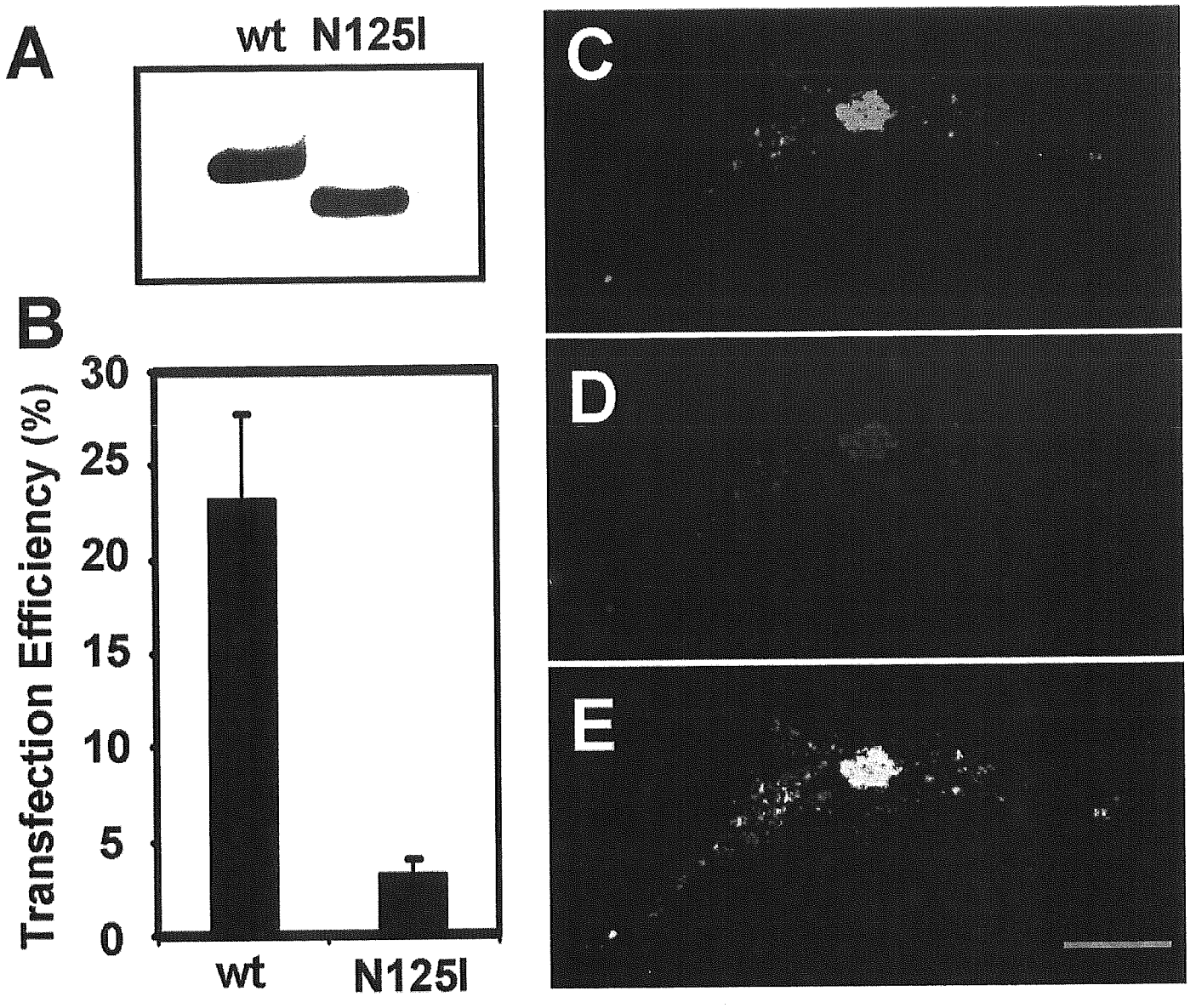
A
wt N125I
B
Transfection Efficiency (%)
30
25
20
15
10
5
0
wt
N125I
C
D
E

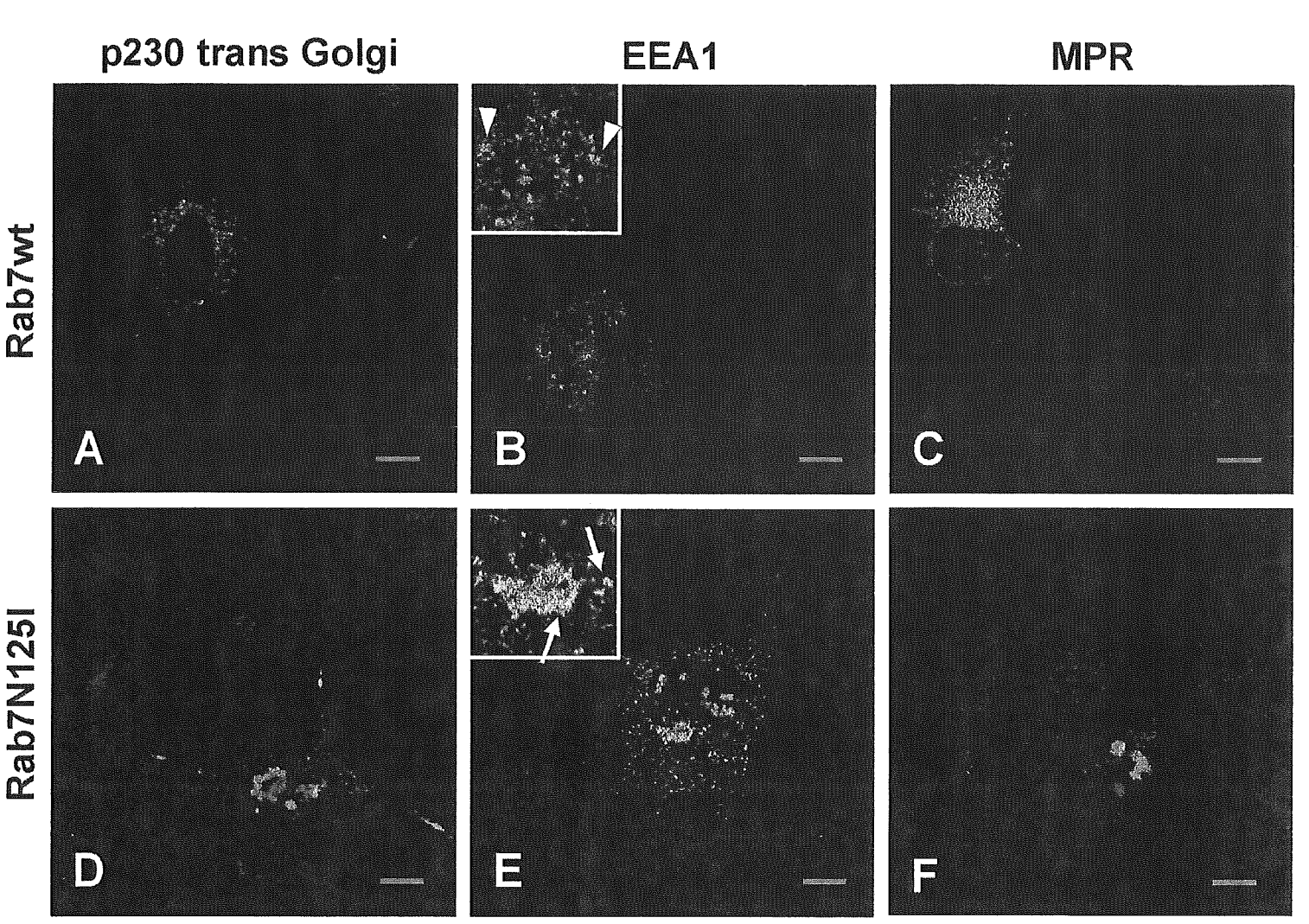
p230 trans Golgi
EEA1
MPR
Rab7wt
Rab7N125I
A
B
C
D
E
F